NOTES AND CORRESPONDENCE

The Southern Oscillation. Part VIII: Model Sensitivity to SST Anomalies in the Tropical and Subtropical Regions of the South Pacific Convergence Zone

HANS VON STORCH
Max-Planck-Institut für Meteorologie, Hamburg, Federal Republic of Germany

HARRY VAN LOON
National Center for Atmospheric Research, Boulder, Colorado*

GEORGE N. KILADIS
Cooperative Institute for Research in Environmental Sciences, Boulder, Colorado

28 January 1987 and 17 July 1987

ABSTRACT

We show by means of a general circulation model experiment that the atmospheric circulation over the South Pacific Ocean is sensitive to sea surface temperature anomalies in the tropical and subtropical regions of the South Pacific convergence zone. The possible implications for understanding the life cycle of an extreme event in the Southern Oscillation are discussed.

1. Introduction

An analysis was performed by van Loon and Shea (1987, hereafter called vLS) of the average sequence of anomalies of sea level pressure (SLP) in the Southern Hemisphere associated with the extreme of the Southern Oscillation (SO) known as a Warm Event. This is the phase of the SO when the Tahiti minus Darwin SLP difference becomes consistently negative, the surface water in the equatorial Pacific is substantially warmer than normal, and unusual rains occur in the normally dry areas on the equator in the Pacific and the coast of Peru. The development of the opposite extreme in the SO, the Cold Event, is in most respects opposite to that of a Warm Event but the anomalies are weaker (van Loon and Shea, 1985).

The vLS analysis showed that the area dominated by the South Pacific convergence zone (SPCZ) plays an important role in the development of anomalies in rainfall, SLP, and wind over the South Pacific Ocean. During the southern spring of the year before a Warm Event the SPCZ expands southwards in its annual cycle over a sea surface which, in the mean, is warmer than normal (vLS). At this stage the mean rainfall in the convergence zone is observed to be higher in the Warm than in the Cold Event, besides being well above normal; and the SLP in the SPCZ is lower in the warm than in the Cold Event, and well below normal also. With the lower SLP, the trades are weaker north of 30°S. van Loon and Shea (1987) suggest that the positive SST anomalies in Year_{-1} of a Warm Event over the region where the SPCZ holds sway are instrumental in weakening the South Pacific subtropical ridge and the trade winds on its north side through their influence on the convection in the SPCZ.

In Year_0 of a Warm Event, the mean anomaly pattern of SLP in early southern winter is the opposite of that 12 months earlier in Year_{-1}, and the SST anomalies in the domain of the SPCZ are now negative. The southward expansion of the SPCZ in the southern spring of Year_0 therefore takes place over anomalously cold water, and the rainfall in the convergence zone is now observed to be below normal while the SLP and the trades west of 150°W are above normal. The negative SST anomalies below the SPCZ thus have the opposite effect of the positive anomalies 1 yr earlier: They strengthen the Pacific ridge in the west and the trades on its north side by supressing the convection in the SPCZ.

To examine this interpretation of the observations suggested by vLS, we test the sensitivity of the SPCZ to changes in the underlying SST by a numerical experiment which is described in section 2. We are interested in finding out whether the model responds to the imposed SST anomaly with a *pattern* resembling

* The National Center for Atmospheric Research is sponsored by the National Science Foundation.

Corresponding author address: Dr. Hans von Storch, Max Planck Institut für Meteorologie, Bundestrasse 55, D-2000 Hamburg 13, Federal Republic of Germany.

that of the atmospheric anomalies observed simultaneously with the SST anomalies. We do not intend to reproduce the atmospheric response in detail. For that reason we use an SST anomaly which is highly idealized in shape and remains unchanged in the course of the experiment. As the experiment is short—for economic reasons—we have used substantially higher values of SST anomalies than those observed, to produce a signal which is clear enough to be distinguished from noise. The experiment is therefore also a study of the reaction of the model's SPCZ to anomalous sea surface temperatures.

2. Design of the experiment

The model used is the T21 version of the ECMWF spectral model discussed by Fischer (1987). Its horizontal resolution is roughly 5° latitudinally and longitudinally. It contains a complete physical process parameterization package. Surface properties over land are calculated prognostically, but SST is prescribed. The model is capable of reproducing the main aspects of the general circulation. In particular, the model shows a realistic seasonal march of the maximum upper tropospheric outflow in the tropics from a position north of the equator during northern summer to the SPCZ area in northern winter. The midlatitude westerlies on the Southern Hemisphere are too weak in the simulation. For this reason the results south of about 45°S are disregarded.

Five runs were made with this model: one control run with climatological SST and four anomaly runs with SST anomalies superposed in the SPCZ area. The control run is a 10-yr continuous integration. For each calendar month a mean field of various quantities was calculated from the control run and used as a "normal" from which to derive the "anomalies" of the experimental runs forced by SST anomalies.

As mentioned in the Introduction, we imposed SST anomalies which are idealized in shape and stronger than observed. The same pattern and strength (2°C) were used in all four experiments. The shape (Fig. 1) was chosen according to vLS's analysis of SST anomalies over the domain of the SPCZ in the southern spring of the year before a Warm Event (see Fig. 4c of vLS).

Two experiments were done with the positive SST anomaly in the SPCZ area, and two with the negative SST anomaly. The anomaly runs were initialized with the conditions of 1 October in two randomly chosen control-run years and run until the end of January. The October results were disregarded in order to allow the GCM to adjust to the anomalous boundary conditions (Washington and Chervin, 1980).

In that way, we obtained two statistically independent mean fields of surface pressure, precipitation, cloudiness, and surface winds for November, December, and January for both the cold and the warm SST anomaly.

3. Response of the GCM

In this section, we discuss the GCM's response to the positive and the negative SST anomaly by means of the difference between the monthly mean of the anomaly experiment and the "normal" obtained from the control runs.

a. The positive SST anomaly

Figure 2 shows the sea level pressure deviation from the "normal" for the two positive SST anomaly experiments. In all six monthly mean maps there is a negative SLP anomaly in an area south of 10°S from about 140°E to 140°W. This recurrent behavior in all months and in both experiments exists in all the other quantities considered. Therefore, we show only the seasonal (NDJ) mean of both experiments.

The signal strengthens with time in both experiments, and this intensification as the season progresses

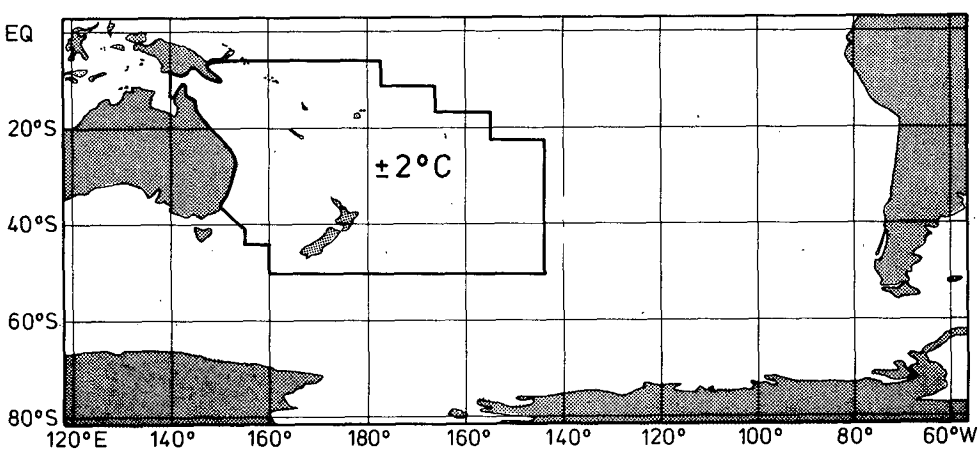

FIG. 1. The pattern of imposed SST anomalies (°C).

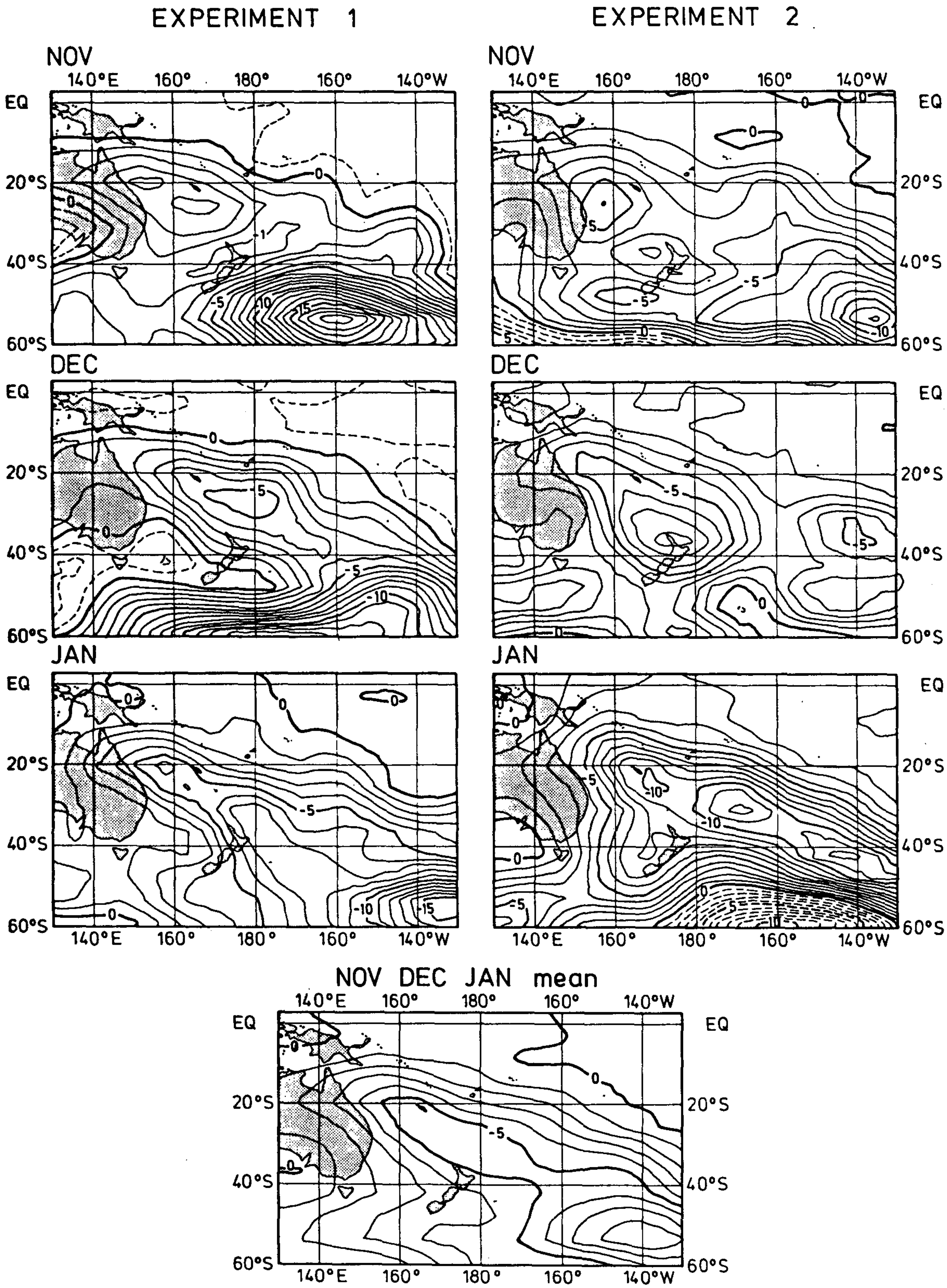

FIG. 2. SLP response (experiment minus control) in November (top), December (middle), and January (bottom), plus the average of all six in the two positive SST anomaly GCM runs. Units: mb. Dashed lines are positive and solid lines negative.

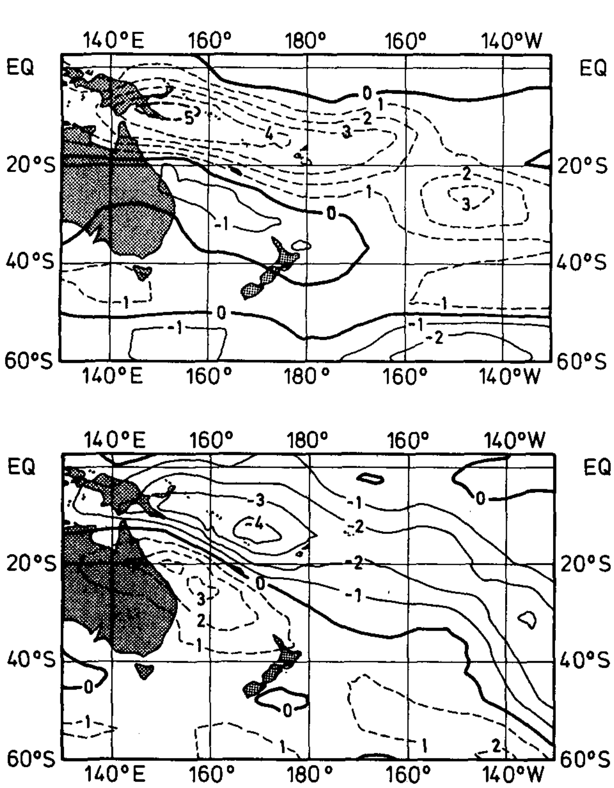

FIG. 3. November–December–January, mean anomalies (experiment minus control) of surface (10 m) wind in the two positive SST anomaly GCM experiments. Zonal (top) and meridional (bottom) components. Average of both experiments. Units: m s^{-1}. Positive anomalies are westerly and southerly.

may be related to the interseasonal change in position of the center of maximum high level divergence in the model as indicated by the 200-mb velocity potential (Bruns and Storch, 1986). In southern winter, this maximum is located north of the equator from where it migrates slowly southward, crossing the equator in spring and reaching its southernmost position in January.

The positive SST anomaly clearly causes the model atmosphere to develop a cyclonic anomaly above the SST anomaly with minimum values between −4 and −12 mb. In the area north of the axis of the SST anomaly there are northwesterly wind anomalies, and south of the axis are southeasterly anomalies. The anomalous meridional and the westerly components are as large as 4–5 m s^{-1}, and the anomalous easterly component is almost 2 m s^{-1} (Fig. 3). On the equator, easterly wind anomalies prevail east of 160°E, and westerlies west of 160°E, with maximum values of 2 m s^{-1} in both November, December and Januarys (NDJs).

The anomalies of the diabatic quantities, cloud cover and convection in Fig. 4, are consistent with the hydrodynamic response of a cyclonic anomaly. Over the northern part of the forcing SST anomaly, a consistent excess of convective rain of as much as 300 mm/month is found, and there is a deficit over most of New Guinea and in the western equatorial Pacific. The pattern in the cloud cover is similar, with anomalies as much as 25% above "normal".

The largest response in rainfall is to the north of the zero line of anomalous wind (Fig. 3). This is the usually observed distribution of rain in the ITCZ with the heaviest rain on the equatorward side of the strongest convergence (e.g., Streten and Zillman, 1984), and it is related to the fact that the flow from the equator is moister and warmer and is in the direction of the convergence of meridians.

In the North Pacific no consistent response is found as might be expected from linear theory.

b. The negative SST anomaly

The response to the negative SST anomaly in the SPCZ area, which is the condition of either a Year_0 in a Warm Event or of a Year_{-1} in a Cold Event, is less marked than the response in the positive SST anomaly runs. This is consistent with earlier findings in GCM sensitivity experiments (Blackmon et al., 1983; Storch and Kruse, 1985). Nevertheless, in either experiment the regional characteristics are quite similar in the three months of November, December, and January.

A consistent maximum value of SLP anomaly of more than +4 mb appears in the experiment with neg-

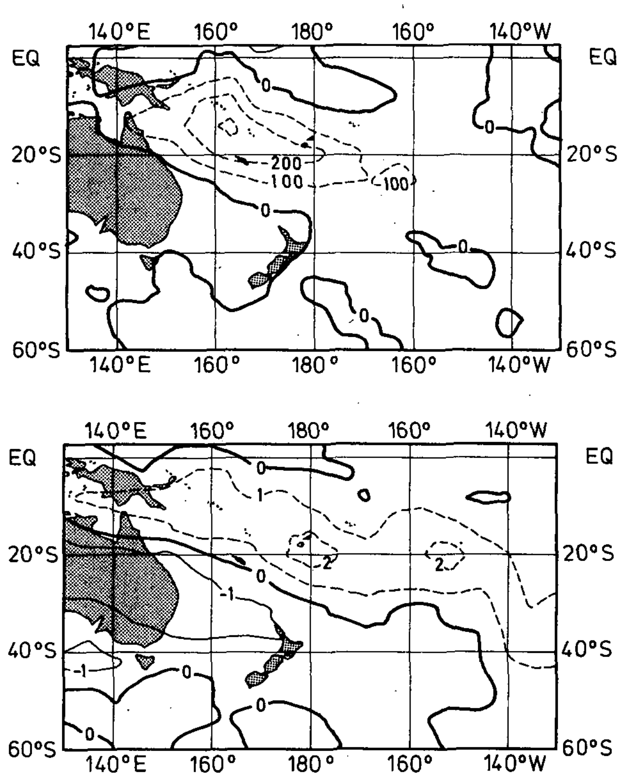

FIG. 4. As in Fig. 3, but for convective rain (top, units: mm/month) and cloud cover (bottom, units: ⅛ coverage).

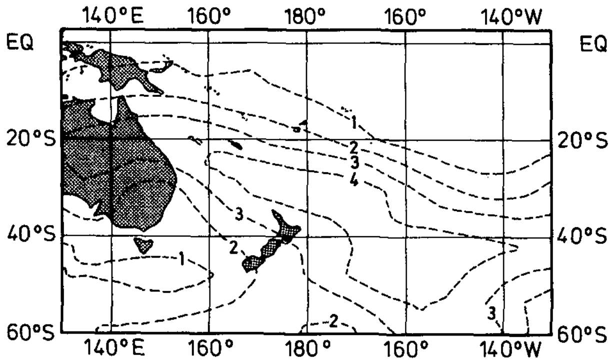

FIG. 5. As in Fig. 2, but for sea level pressure simulated in the negative SST anomaly experiments.

ative SST anomalies (Fig. 5). This response and the 10 m surface wind response have a pattern similar to that in the positive SST anomaly experiments but with the opposite sign and somewhat lower maximum values. Such a reversed and slightly weaker pattern is also found in the rainfall anomalies: over the northern part of the negative SST anomaly the average deficit is 150 mm/month, whereas on the equator there is an excess of 100 mm/month (not shown).

An interesting aspect of the warm-anomaly experiment may be inferred from the similar anomaly patterns in the cold and warm anomaly experiments. Adding 2°C to the mean SST raises it to 30–31°C over the northern parts of the area. One might think that the response was simply the result of these high SSTs, which are as high as any observed ones could possibly be; but because lowering the mean to about 26°C in the cold-anomaly experiment, which is not an extreme low, still produces the same anomaly pattern, we may deduce that the model is not overreacting to the near equatorial warm anomaly.

At the southern edge of the SST anomalies the values are much larger than the observed ones. This part of the pattern is, however, only marginally relevant, as GCM experiments that test the sensitivity of the atmosphere to midlatitude SST anomalies have shown (Hannoschöck and Frankignoul, 1985). The abrupt change of anomaly from 2°C to 0°C at the edge poses no problem to the model (e.g., Keshavamurt, 1982). Owing to the discretization, even steeper gradients of surface temperature appear at the coastlines in the model.

c. Consistency with observations

The response of the model to the negative and positive SST anomalies thus has a similar pattern but opposite sign. We now compare the GCM results with the observed difference between NDJ-composites (Kiladis and van Loon, 1987) of the year before Warm, and the year before Cold Events (Figs. 6 and 7). The mean precipitation and sea level pressure during NDJ_{-1} were calculated at each station for warm events, using all available data. Thus, the number of events does vary from station to station. The same was done for Cold Events. The composite mean for the Cold Event was then subtracted from the composite mean for the Warm Event, giving the composite difference. If a station had less than five Warm Events or less than five Cold Events in its record, it was eliminated from the analysis. The differences were then mapped.

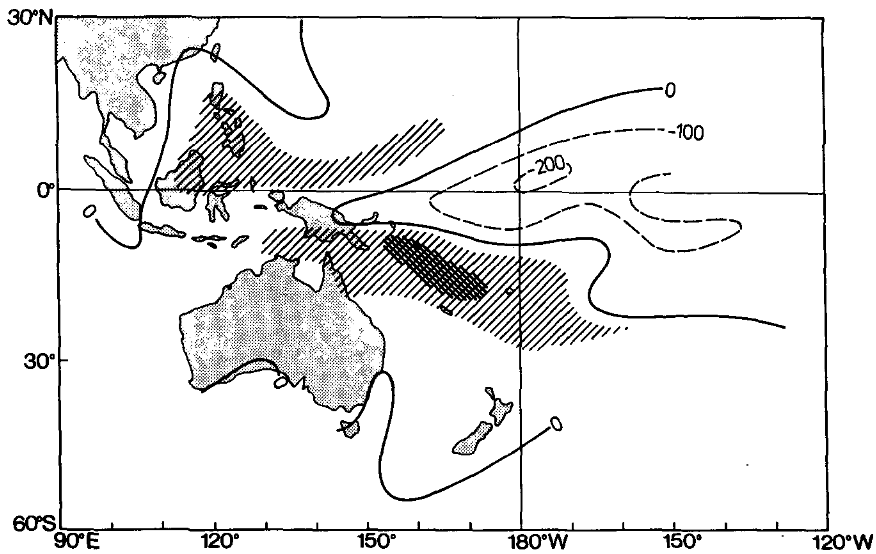

FIG. 6. November–December–January, mean difference of observed precipitation (mm/month) between the year before a Warm Event and the year before a Cold Event. The map is based on long-term series of station reports. The area with a precipitation difference of more than 50 mm/month is hatched, crosshatched above 100 mm/month.

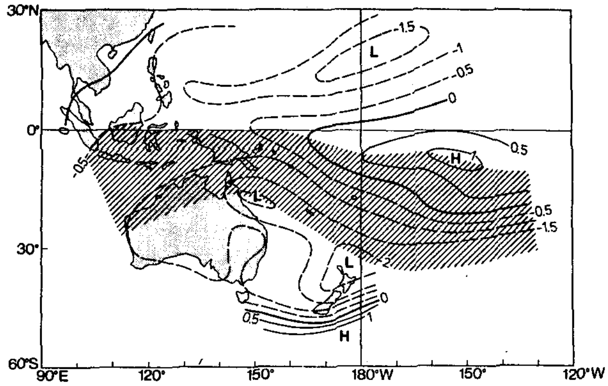

FIG. 7. As in Fig. 6, but for observed sea level pressure (mb). The area with anomalous westerly geostrophic wind south of the equator is hatched.

We cannot expect the size of the observed and modeled anomalies to be identical since we used an enhanced SST anomaly in the GCM. Also, one might expect differences with respect to details in the patterns, associated with systematic errors in the GCM owing to sample fluctuations in the model and in the observed data, and to the idealized pattern of the SST anomaly. The gross pattern and sign should be the same in simulation and observation, however, if the vLS hypothesis outlined in the Introduction is a valid one.

The simulated (Fig. 4) and observed (Fig. 6) composited rainfall anomalies are similar: Both show an excess of rainfall in the area between 10°S, 160°E and 20°S, 180°E and farther southeastward. The maps also share a deficit of rainfall west of the dateline on the equator. Here, the largest observed deficit is about 240 mm/month, which is twice the highest observed excess of 100–150 mm/month farther south. In the model, the positive SST causes an increase of rainfall of 250 mm/month, but a much weaker decrease on the equator. This difference is likely due to the fact that in the GCM experiment SST anomalies force the overlying atmosphere only in the region of the SPCZ, whereas in reality, there are also SST anomalies along the equator but of the opposite sign.

The observed SLP composite difference (Fig. 7) is qualitatively in accord with the simulated SLP response (cf. Figs. 2 and 5). The increase of SST in the region of the SPCZ results in a decrease of pressure over the region, and conversely for a decreased SST.

4. Conclusion

An analysis (van Loon and Shea, 1987) of the SO on the Southern Hemisphere demonstrated that the annual cycle of the South Pacific Convergence Zone affects the development of the extremes in the SO. It was suggested by vLS that the atmospheric anomalies in the SPCZ (in pressure, wind, and rain) are associated with temperature anomalies in the sea surface below the SPCZ. The model experiment which we have described above is designed to test the sensitivity of the convergence zone to changes in the sea surface temperature. The position and the sign of the SST anomalies are correct in the model, but their intensity and spatial and temporal uniformity are not as observed.

Our experiment shows that changes in the temperature of the underlying sea surface do affect the position and intensity of the SPCZ. Over the anomalously warm water imposed in the domain of the SPCZ, the rainfall in the model increases, the pressure falls, and anomalous westerlies are widespread in the trades and west of 160°E on the equator. Anomalies of the opposite sign, but weaker, appear when negative SST anomalies are imposed.

The outcome of the experiment thus agrees with vLS's interpretation of the observations, but such favorable results are not surprising. Palmer and Mansfield (1984), e.g., have postulated that large SST anomalies over a warm water surface in a zone of convergence would enhance (warmer water) or suppress (cooler water) convection. Otherwise, the experiment is interesting because it tests what may be necessary (but not necessarily sufficient) precursors to the extremes of the Southern Oscillation, and because it deals with SST anomalies outside the equatorial belt which evoke a well-defined response that is physically easy to understand. Interesting as the equatorial anomaly experiments are, they deal with a stage in the Southern Oscillation when an extreme has almost run its course, and therefore they do not tell us about the development of the extremes in the SO, although they do serve to explore the predictive skill inherent in equatorial SST anomalies in the Pacific Ocean.

Acknowledgments. We are grateful to Dorene Howard, Ulla Kircher and Ilka Brecht, who processed the manuscript, and to Marion Grunert and Doris Lewandowski, who prepared the diagrams. We thank Dr. Edilbert Kirk, Ulrich Schlese and Ingo Jessel, who performed the model runs and their diagnoses.

REFERENCES

Bruns, T., and H. von Storch, 1986: Performance of the ECMWF-T21-GCM in the tropics. *Research Activities in Atmospheric and Oceanic Modelling,* Report **9**, G. J. Boer, Ed., World Meteorological Organization, WMO/TD, 141 pp.

Blackmon, M. L., J. L. Geisler and E. J. Pitcher, 1983: A general circulation study of January climate anomaly patterns associated with interannual variation of equatorial Pacific sea surface temperatures. *J. Atmos. Sci.,* **40,** 1410–1425.

Fischer, G., 1987: Climate simulations with the ECMWF T21 model in Hamburg. *Large Scale Atmospheric Modeling Report* **1,** Meteorologisches Institut der Universität Hamburg, Bundesstraße 55, 2000 Hamburg 13, FR Germany, 159 pp.

Hannoschöck, G., and C. Frankignoul, 1985: Multivariate statistical analysis of a sea surface temperature anomaly experiment with the GISS general circulation model. *J. Atmos. Sci.*, **42**, 1430–1450.

Keshavamurti, R. N., 1982: Response of the atmosphere to sea-surface temperature anomalies over the equatorial Pacific and the teleconnections of the Southern Oscillation. *J. Atmos. Sci.*, **39**, 1241–1259.

Kiladis, G. N., and H. van Loon, 1987: The Southern Oscillation. Part VII: Meteorological anomalies over the Indian and Pacific sectors associated with the extremes of the Oscillation. *Mon. Wea. Rev.* (in press).

Palmer, T., and D. A. Mansfield, 1984: Response of two general circulation models to sea surface temperature anomalies in the tropical East and West Pacific. *Nature*, **310**, 483–485.

Storch, H. von, and H. A. Kruse, 1985: The extra-tropical atmospheric response to El Niño events-a multivariate significance analysis. *Tellus*, **37A**, 361–377.

Streten, N. A., and J. W. Zillmann, 1984: Climate of the South Pacific Ocean. Climate of the Oceans, Vol. 15, H. van Loon, Ed., 263–429, Elsevier, Amsterdam.

van Loon, H., and D. J. Shea, 1985: The Southern Oscillation. Part IV: The precursors south of 15°S to the extremes of the oscillation. *Mon. Wea. Rev.*, **113**, 2063–2074.

——, and ——, 1987: The Southern Oscillation. Part VI: Anomalies of sea level pressure on the Southern Hemisphere and of Pacific sea surface temperature during the development of a warm event. *Mon. Wea. Rev.*, **115**, 370–379.

Washington, W. M., and R. M. Chervin, 1980: Response time of an atmospheric general circulation model to changes in ocean surface temperature: implications for interactive large-scale atmosphere and ocean models. *Tellus*, **32**, 119–132.